Solid Freeform Fabrication 2023: Proceedings of the 34th Annual International Solid Freeform Fabrication Symposium – An Additive Manufacturing Conference
Reviewed Paper

INVESTIGATION OF INSTRUMENTING ROBOCASTING PRINTER FOR CERAMIC SLURRIES

J. McCleary[1]*, N. Durand[1], L. Castillo Perez[1], G. Medina Zorrosa[1],
J.P. Garcia Chavira, D. Espalin[1]

[1] The University of Texas at El Paso, El Paso, TX 79968, USA;
[1] W.M. Keck Center for 3D Innovation, El Paso, TX 79968, USA;
* Corresponding author (jamccleary2@utep.edu)

Keywords*: In-situ monitoring, Robocasting, Ceramics, Quality control*

ABSTRACT

Robocasting has multiple steps from ceramic slurry preparation to sintering that can impact the end part quality. In-situ monitoring and process controls can aid in minimizing differences in the quality of printed parts. The study and impact of different parameters during the printing process and a parameter database will improve the quality between green bodies and sintered parts. This paper discusses implementation of a CMOS camera, dynamic pressure sensor, and 2D laser scanner into a custom-built robocasting printer for in process monitoring. Single line beads were printed and analyzed by measuring the dimensions and pressure changes during printing. Results show that the printer with sensors detected the location of possible defects and changes in printed samples but further investigation is needed to filter noise and collect conclusive data.

1 Introduction

Robocasting is a 3D printing process that selectively deposits a slurry through a nozzle in a layer-by-layer fashion wherein the slurry consisting of ceramic particles and organic additives.[1] Many aspects seen in robocasting cause difficulties when creating ceramic parts for commercial use. Studies have shown that material formulation, environment, printing parameters, and post processing impact the outcome and final properties of printed parts.[2] For this reason in-situ monitoring, quality assurance and control are essential to bolster the future growth of ceramic AM. It was reported at a workshop by the National Institute of Standards and Technology (NIST) that development of rapid and cost-effective non-destructive techniques for quality control would

improve the commercialization of ceramic AM. Also, the need for standardized characterization, modeling, and curated databases for feedstock properties, AM build processes, and as-built green-body material properties are important areas of study.[3]

Research has been conducted by Michael Mason with a ram extruder for high solid loadings paste by applying an on-line extrusion force controller that measured force and changed ram velocity to enable fabrication of parts previously not possible due to slow response times of ram extruders.[4] Other experiments have been conducted to try and improve the precision of the start and stop events for three styles of extruders used in ceramic AM.[5] The results showed that the auger screw extruder performed the best, based on measurements that were analyzed by imagej imaging software. Ram extruder's printing process has been modeled and attempted to improve the start and stop of extrusion by introducing dwell time and controlled force during extrusion. Results showed the dwell control at start and stop essential, and it also noted that further study into velocity profile along the extrusion path necessary to eliminate excess accumulation at the start of extrusion.[6] Experimental modeling has been conducted and the printing height based on nozzle diameter along with rheological characteristics of paste to include drying kinetics are key parts for proper modeling of paste extrusion and dimensionally accurate printed samples.[7,8]

Research has also been conducted on a mid-IR OCT as a tool for quality assurance, at-line for 3D ceramic printing and provided a way to investigate various structural features and defects by non-destructive methods. [9] Laser powder bed fusion (LPBF) has been on the cutting edge when trying to in-situ and in-line monitor the AM process from start to finish. Yoa Chen reported on recent technologies used in metal AM for defect detection that covered penetration, eddy current, infrared imaging, and ultrasonic defect detection.[10] When investigating ceramic AM many of these methods for defect detection are unsuitable due to the porosity, surface roughness, or nonconductive nature of some ceramics used when trying to inspect green bodies.

To allow for instrumentation for in situ and in line monitoring, the W.M. Keck Center for 3D Innovation designed and manufactured a ceramic 3D printer that was intended to study the impacts of environmental conditions and aid in developing a database for the printing process of ceramic materials. For this paper a CMOS camera, laser scanner, and dynamic pressure sensor were fitted to the printer to investigate if in-situ and in-line monitoring of individual printed beads were possible.

2 Printer design

Industrial level AM machines tend to have limited to no customization available to firmware and hardware without costly and time-consuming modifications, in some cases voiding the warranty. Desktop 3D printers are either closed or open source but still have limited upgradeability without completely replacing multiple components from the existing system. Also, modifying an existing printer for ceramic extrusion and instrumentation the size of the printer is normally designed for a specific tool head. Earlier robocasting tests were conducted by this team using a Lulzbot Taz 6 that had a relay board attached to its IO pins to toggle on/off a Nordson EFD

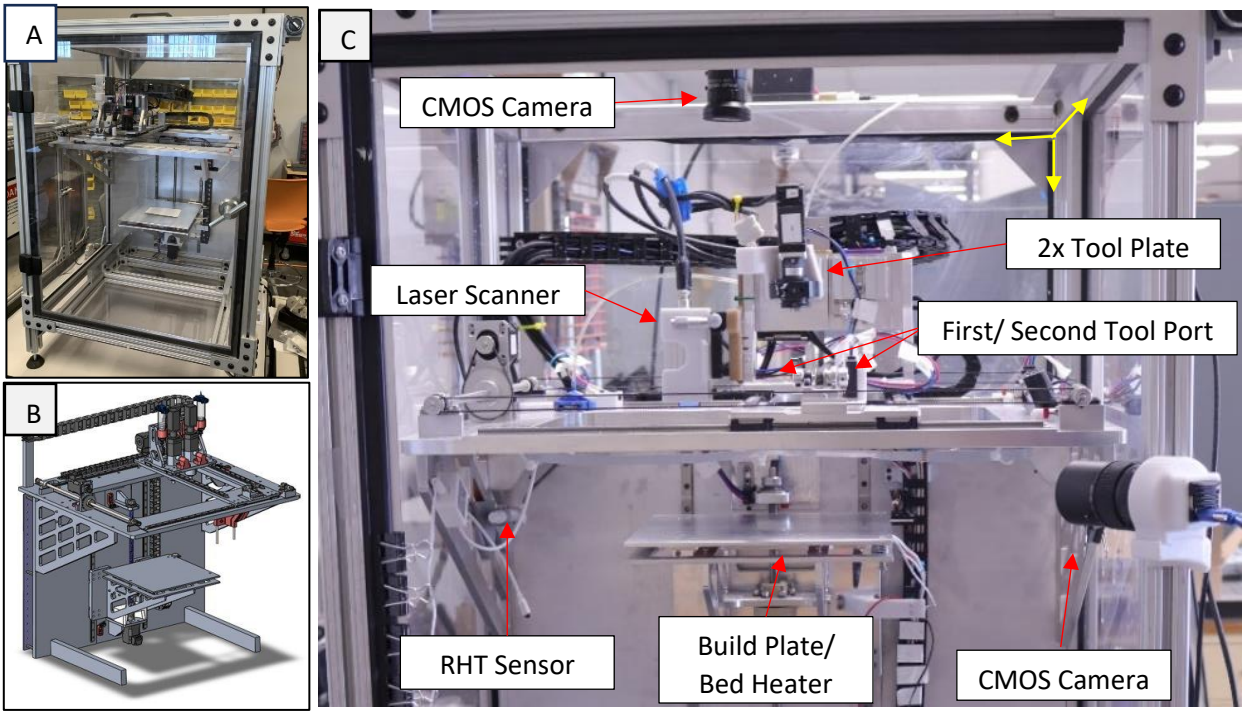

Figure 1 (A) Fully encosed printer after assembly (B) CAD model of major components for motion system (C) Instrumentation mounted on printer configuration for experimentation without extruder mounted

auger tool. The Lulzbot Taz 6 had a limited number of IO pins and limited space available to add multiple sensors for monitoring prints.

A printer reported on here for robocasting (figure 1A) was custom built to be expandable and focused around the VIPRO-Head3 auger tool (ViscoTec, Kennesaw, GA) for extrusion. It was designed with a primary and secondary tool port for an additional auger tool or other tooling method as needed. This functionality is enabled by quick tool changing plates and an expandable electrical system that supplies single phase 120V AC, 24V DC, 12V DC and 5V DC power sources. The printer's firmware was developed in Parker Automation Manager v1.4.0 (PAM) and ran on a Parker Automation Controller (PAC320) (Parker Hannifin, Cleveland, OH) that has three IO modules; an analog output module that supports up to four 0-10 V or 4-20 mA signals, an analog input module that supports up to eight single-ended or four differential 0-10 V inputs, and a digital input output module that supports up to 16, 24V 0.5A signals each. The PAC320 allows for up to 32 IO modules which enables continued and easy expansion when necessary. The PAM allowed for completely customizable user interface (UI) that is quickly changed to allow for additional tools or instrumentation functionality. Most of the functionality in the UI was programmed by the user using function blocks and structured text found in IEC Section 61131-3 Standard.

The printer was also designed to regulate and monitor the temperature and humidity of the printing environment. All components used in the design of the printer can sustain 80% humidity for extended periods of time, and the chamber around the printer was sealed to allow for control

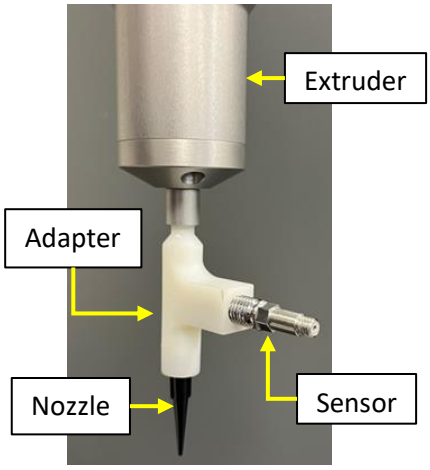

Figure 2 Model 113B27 Pressure Sensor with housing adapter

of the printer environment. The printer also has a heated bed that has previously been found useful for drying layers of printed samples. Both features were not used in this paper during instrumentation.

During the creation of this manuscript, the printer was configured with two Alvium 1800 U-2050 CMOS cameras (Allied Vision, Stadtroda, Germany) and a scanControl LLT 3010-50 2D/3D Profile sensor (Micro-Epsilon, Raleigh, NC).The laser scanner has a z-axis resolution of 3 microns and x-axis resolution of 12 microns while the cameras have a resolution of 20 MP. Additionally, it had an ICP Pressure Senor model 113B27 (PCB Piezotronics, Depew, NY) that was attached to the auger tool during printing (figure 2). The pressure sensor has a sensitivity of 7.25mV/kPa, resolution of 0.007 kPa and non-linearity of less than 1%.

3 Methodology

3.1 Printer Calibration

Accuracy and precision needed to be determined for the printer with different sensors and measurement devices to confirm that data could be reliably interpreted. The laser scanner was mounted to the printer as shown in figure 1C and scanControl Configuration Tools 6.7 software was used to manually scan gauge blocks while jogging the x and y-axis. The standoff distance was calibrated by using the front facing CMOS camera and two-gauge blocks measuring 2.54 mm and 2.64 mm. The CMOS camera was used to determine the exact moment that the nozzle tip touched the 2.64 mm gauge block. The block was then replaced with the 2.54 mm gauge block and the nozzle were moved into direct contact with the 2.54 mm gauge block using the CMOS camera. This height difference was then recorded from the UI on the computer, and the calibration was performed five times to determine the average and standard deviation of the results. Based on these results, the CMOS indexing process was determined to vary on average by 15 µm, thus validating the standoff process for experimentation.

The bed was leveled using a dial indicator to 30 microns across the length in y-axis and 10 microns across the length of the x-axis. Scaling and mapping were done using the PAM software using the gear ratios and verified by indexing at the end of travel across each axis to 99.01%

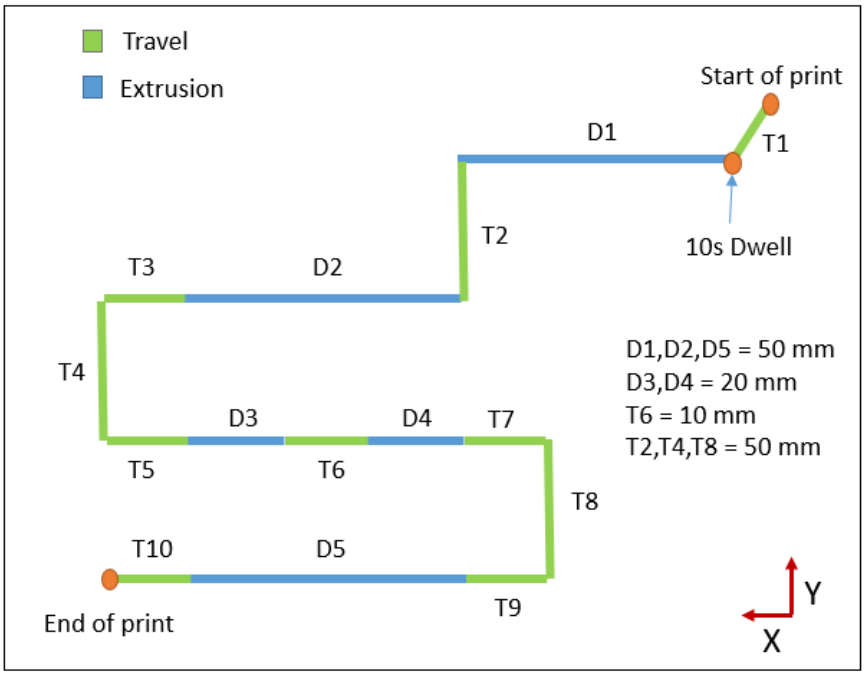

Figure 3 Pathing and extrusion created with custom GCODE to study specific events with sensors

accuracy which equated to excess travel of 2.5 mm across a 250 mm distance. The CMOS camera is intended to take top-down image of layers and study drying of samples overtime. A python script was written to measure objects and the scaling factor used in the script was calculated by imaging 31 separate gauge blocks ranging in widths (1.27 mm to 12.7). This allowed for a sample length and width to be calculated with a standard deviation of 0.83%.

3.2 Single Bead Experiments

Individual ceramic beads were printed to determine if observations of the start, stop and continuous flow events can be detected and identified by the sensors. Parameters were changed to determine if different signatures could be identified. This was done by writing a custom GCODE to limit the impact of commercially available slicers and prevent modifying multiple parameters when changes are made to individual parameters. The custom GCODE pathing shown in figure 3, allowed for the study of continuous flow in extrusion D2 and D5. Extrusion D3 and D4 are gapped by a 10 mm spacing to study the effects of rapid start and stop events. The travel in y-axis were all 50 mm to simulate a longer delay between extrusions.

A second line test was conducted to study laser scans over time to see if impacts of single bead settling was detectable. This test was conducted by printing a single bead 50 mm in length with a 0.4 mm standoff height, 0.84 mm inner diameter nozzle, 10 mm/s print speed.

The dynamic pressure sensor was located just above the nozzle and after the paste leaves the auger tool. The pressure sensor is connected via a custom housing printed on a vat photopolymerization printer. Test were conducted with and without the pressure sensor attached and motor traces were tracked when test were conducted using the pressure sensor.

3.3 Data Acquisition and Curation

During the printing process measurements from the dynamic piezoelectric pressure sensor were collected in real time by a data acquisition tool using MATLAB with a separate computer from the printer. This was due to the pressure sensor needing a high-definition audio card to collect the data from the sensor. The existing computer running the printer firmware and CMOS camera did not have the necessary sound card receive the sensor data. The communication between the computer and sensor was enabled by a signal conditioner model 485B39 (PCB Piezotronics, Depew, NY).

The Laser scanner scans were collected using scanControl Configuration Tools at 10 mm/s and 400 profiles a second and processed using scanCONTROL 3D view (Micro-Epsilon) to convert the scan file into excel for further analysis using MATLAB. The excel file from scanControl was ran through a MATLAB code to determine the height, width, and area across the length of the printed bead. Due to placement of the laser scanner scans could only be conducted across the length of the y-axis. The build plate that was used for the custom GCODE needed to be repositioned after printing to perform scans. The single line settling scans were scanned at 30 second time intervals immediately after deposition without any user interactions.

The overhead CMOS camera was initially attached to the second tool port and manually jogged over each printed bead. Images were captured using Vimba Viewer X software from Allied Vision and processed using a Python script using OpenCV and Numpy libraries to determine if the width and length of the bead could be accurately determined. The position of the camera was later moved to a fixed position at the top of the printer enclosure. The side facing CMOS camera was only used for indexing the nozzle onto the build platform. Images were captured from 12.7 mm diameter disk from above at 30 second time intervals for 10 minutes using a trigger from the UI.

Motor commanded, actual position and velocity signatures were able to be seen by exporting a csv file from PAM after printing that was tracked by the drivers of the motors in real time. Only a limited number of motor signatures could be recorded at a time due to the limited number of commands that could be processed by the PAC320 to run the printing sequence and collect data from the drivers at the required rate.

4 Results and Discussion

4.1 Pressure sensor

A sample of the data collected and plotted using MATLAB is shown in figure 4 that also shows the actual extrusion motor traces collected from the motor drivers for commanded on and off marked by vertical lines. The signal shows peaks and valleys in the signal that corresponds to the five commanded extrusion events. The peaks and valleys were consistent across all prints showing the location of the start and stop of extrusion could be identified by the pressure sensor. Actual extrusion of paste happened right near the peak of each signature, while the stop of extrusion would happen right before reaching the minimum point of the valley. If an extrusion event or time between extrusion was long enough the signal would recover and normalize, this is

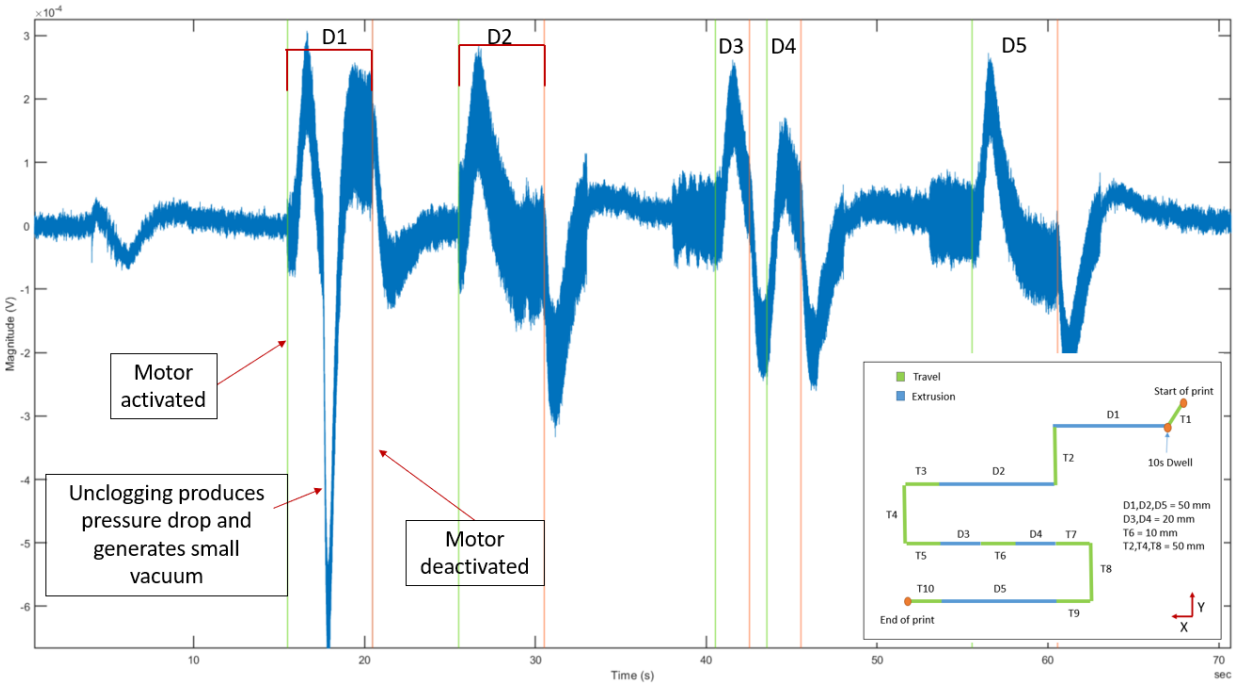

Figure 4 Pressure signal with green and red vertical lines to show actual extrusion motor activation and deactivation respectivily. Pathing shown for reference

seen in the space between the end of D2 and start of D3. When looking at D3 to D4 there is no time for the signal to normalize but both start and stop events can be identified from the signatures. D2 and D5 have similar signatures, except just before the start of D5, there is noise in the signal that is distinct from x-axis travel movements that would correspond to T9 travel which can again be seen at T5 just before D3. Further testing is needed to determine the exact reason for the noise and the source causing the distinct signature in the signal.

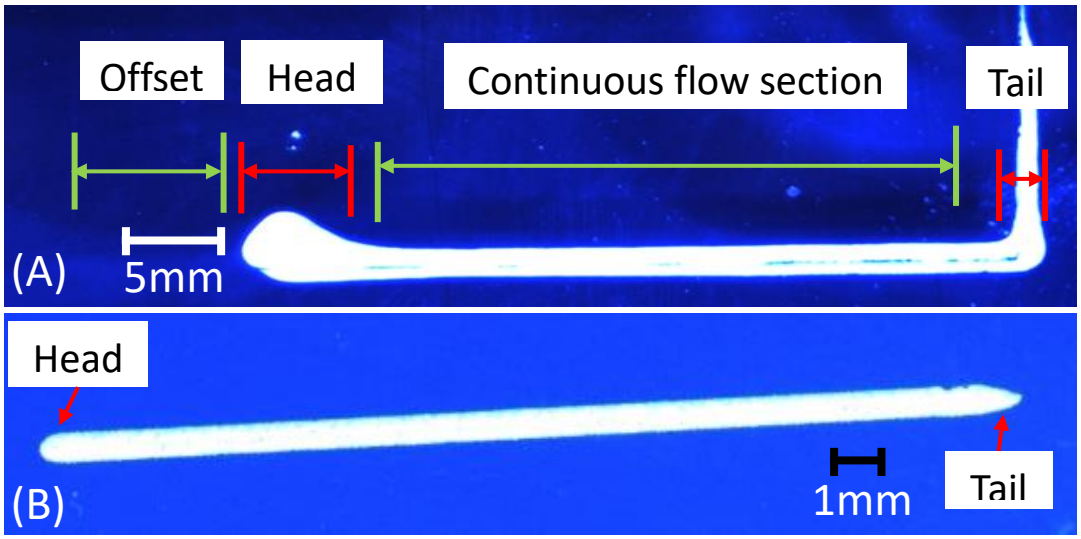

Figure 5: Printed beads captured with CMOS camera (A) 50 mm single bead printed with pressure adapter housing (B) 20 mm single bead printed without pressure adapter housing

Extrusion D1 has a unique signature and is normally referred to as the purge line during testing. While the magnitude of the peak for D1 in Figure 4 is similar to the magnitude of other peaks, this is not consistent with all data. The valley for D1 also has a greater minimum when comparing to the other extrusions seen in Figure 4. The suspected reason for this signature is the extruder is idle for an extended period before printing due to operational setup and different users. The idle is normally only 1-3 minutes before printing but the time has currently not been tracked to confirm the impact on the signal. In Figure 5A a single bead with a large offset and oversized head is shown that would correspond to a large peak in a pressure signature. Also, seen in Figure 5 is a comparison of a printed bead that was printed using the pressure sensor adapter attached and a printed bead without the pressure sensor adapter attached.

While many events were able to be identified by the pressure sensor further test need to be conducted to confirm anomalies and defects can be properly identified without impacting the printing process through instrumentation. It is believed that the large internal volume of the adapter housing for the sensor had a negative impact on the printing process. The auger tool was selected because the screw driving the material allows for a quick response unlike a ram or pressure driven syringe. The adapter housing was causing a delayed response at the start and stop of extrusion and discontinued so the effects of printing parameters could be investigated. Future work will be put into redesigning the pressure adapter housing to lower the response impact.

4.2 Laser Scanner

The 2D laser scanner is attached to the side of the y-axis tool carriage with a pan and tilt enabled mount. The placement of the sensor is due to a requirement that the base of the scanner be

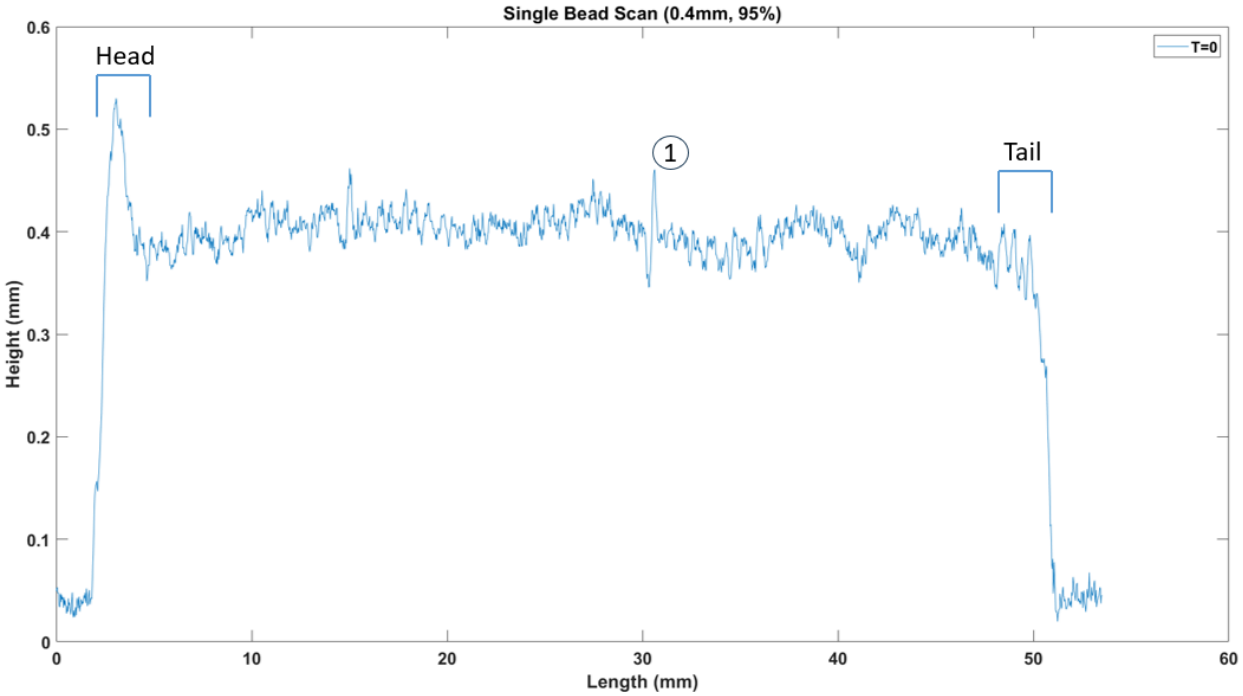

Figure 6: Graph of maximum height data collected from 3D scan plotted using MATLAB, printed bead had a 0.4 mm stand off distance and 95% flow base on a control value with traversing speed 10 mm/s. Head and tail section shown only for orientation, point 1 shown for reference point of interest

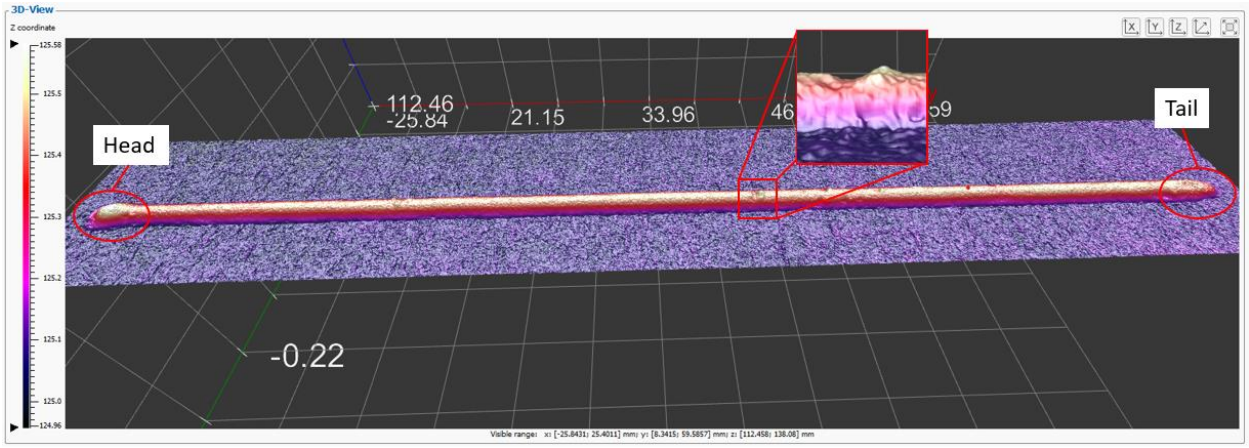

Figure 7: 3D view of scan data shown in Figure 6 displayed in scanCONTROL 3D-View, Head and Tail section circled for reference. Enlarged image corresponds to drop and large spike in height seen in Figure 6 reference point 1

between 105 mm – 145 mm while 125 mm is the optimal scanning distance. This placement reduced the print area in the x-axis by 80mm but allowed for the sensor to be attached for automated scanning and raising and lowering the build plate for the optimal scanning distance. In this orientation the laser scanner is only able to scan individual beads that are parallel with the y-axis or the build plate would need to be rotated 90^{o} before scanning.

Data collected by scanControl Configuration Tools allowed for individual profiles to be viewed and analyzed but was a time-consuming process. While a full 3D view of data could be shown in scanControl 3D view software it still lacked a way to quickly model data for easy analysis mathematically. Instead, the data was collected and analyzed using a MATLAB code to measure the width, height, and area over the length of a single bead. Figures 6 and Figure 7 show the same sample bead in MATLAB and scanControl 3D view respectively. It was demonstrated that using the laser scanner and software in combination that the dimensions of the could be identified and analyzed. The graph shown in Figure 6 displays only the maximum value for each individual profile of a scan. The width and area data are not shown but are necessary to develop a complete understanding of the bead when drawing conclusion from the data. Further testing and analysis are needed to correspond each printing parameter to results, but initial data shows that that standoff distance has significant impact on the bead dimension along with the rheology characteristics of the paste.

5 Conclusions

A custom ceramic paste printer was designed and built to enable future study of various printing parameters. This paper identified three sensors that were able to be incorporated into the printer to study ceramic extrusion in future studies. It was demonstrated that the sensors can be integrated into the system and collect data from printed samples. The pressure sensor showed signals that align with commanded start and stop of the stepper motors. It was also demonstrated that the adapter for the pressure sensor had a negative impact on the printing process and needs to be improved for future work. The laser scanner enabled gathering data about area, width, and height of single beads while sacrificing a small portion of the print area. It will be used in future work along with the CMOS camera to further investigate the settling effects of printed beads. The

CMOS camera in this work was only utilized for indexing the build plate and capturing high quality images for reference.

6 Acknowledgement

The research described here was performed at The University of Texas at El Paso (UTEP) within the W.M. Keck Center for 3D Innovation (Keck Center). The authors are grateful to UTEP students Angel Vega, Luis Banuelos, and Luis Castillo Perez for aiding in the design, manufacturing, and programming of the printer used this paper. Other UTEP students the authors would like to thank are Abigail Ortega, Adrian Duran, Naily Estrella Delgado, Emily Trillo, Carlos Rodriguez and Joshua Carrillo for aiding in instrumentation, data collection, and printing of samples for this paper. The team would also like to Amy Elliot of Oak Ridge National Laboratories, Yirong Lin of The University of Texas at El Paso, and Monsuru Ramoni for their input in the development of this machine and its instrumentation. The authors are thankful to the support from the Department of Energy National Nuclear Security Administration under Award Number DE-NA0004018.

References

[1] M. Rahaman, “Ceramic processing”. 2nd edition, Taylor & Francis Group, 2017.

[2] S. Lamnini, H. Elsayed, Y. Lakhdar, F. Baino, F. Smeacetto, E. Bernardo “Robocasting of advanced ceramics: ink optimization and protocol to predict the printing parameters – a review” *Heliyon,* Vol 8, No. 9, 2022.

[3] A. Allen, I. Levin, S. Witt “Materials research & measurement needs for ceramic additive manufacturing”. *Journal of the American Ceramic Society*, Vol.103, No. 11, pp 6055-6069, 2020.

[4] M. Mason, T. Huang, R. Landers, M. Leu, G. Himas “Aqueous-based extrusion of high solids loading ceramic paste: Process modeling and control” *Journal of Materials Processing Technology,* Vol. 209 No. 6, pp 2946-2957 2009.

[5] W. Li, A. Ghazanfari, M. Leu, R. Landers “Extrusion-on-demand methods for high solids loading ceramic paste in freeform extrusion fabrication”. *Virtual and Physical Prototyping*, Vol. 12, No. 3, pp 193-205, 2017.

[6] T. Oakes et al., "Development of Extrusion-on-Demand for Ceramic Freeze-Form Extrusion Fabrication," Proceedings of the 20th Annual International Solid Freeform Fabrication Symposium (2009, Austin, TX), pp. 206 - 218, University of Texas at Austin, Aug 2009.

[7] H. Fuwen, T. Mikolajczyk, D. Yurievich Pimenov, M. Kumar Gupta "Extrusion-Based 3D Printing of Ceramic Pastes: Mathematical Modeling and In Situ Shaping Retention Approach" *Materials,* Vol. 14, No. 5: 1137, 2021.

[8] J. Wang, L. Shaw “Rheological and extrusion behavior of dental porcelain slurries for rapid prototyping applications”. *Materials Science and Engineering: A*, Vol 397, Iss 1-2 pp 314-321, 2005.

[9] I. Zorin, D. Brouzek, S. Geier, S. Nohut, J. Eichelseder, G. Huss, M. Schwentenwein, B. Heise “Mid-infrared optical coherence tomography as a method for inspection and quality assurance in ceramics additive manufacturing”. *Open Ceramics*, Vol. 12, 2022.

[10] Y. Chen, X. Peng, L. Kong, G. Dong, A. Leach “Defect inspection technologies for additive manufacturing”. *International Journal of Extreme Manufacturing*, Vol. 3, 2021.